

Ion irradiation of carbon nanotubes encapsulating cobalt crystals

O. Lehtinen^{a,*}, L. Sun^b, T. Nikitin^c, A.V. Krasheninnikov^{a,d}, L. Khriachtchev^c,
J.A. Rodríguez-Manzo^e, M. Terrones^e, F. Banhart^b, J. Keinonen^a

^aAccelerator Laboratory, University of Helsinki, P.O. Box 43, FI-00014 Finland

^bInstitut für Physikalische Chemie, Universität Mainz, D-55099 Mainz, Germany

^cLaboratory of Physical Chemistry, University of Helsinki, P.O. Box 55, FI-00014, Finland

^dLaboratory of Physics, Helsinki University of Technology, P.O. Box 1100, FI-02015, Finland

^eAdvanced Materials Department, IPICYT, Camino a la Presa San José 2055, Col. Lomas 4a. sección, 78216 San Luis Potosí, Mexico

Received 26 May 2007; accepted 12 July 2007

Available online 31 July 2007

Abstract

The response of multi-walled carbon nanotubes encapsulating Co nanorods to ion irradiation was studied. The irradiation experiments with medium ion energies (40–500 keV) were carried out at high temperatures and combined with transmission electron microscopy and Raman characterization of the irradiated samples. Contrary to electron irradiation and high-energy (100 MeV) ion irradiation, we did not see accumulation of pressure inside irradiated nanotubes. We found that nanotubes with Co nanorods inside were transformed to amorphous carbon rods encapsulating Co clusters with typical diameters of 3–6 nm. As Co is magnetic, such one-dimensional composite systems could be used for various applications such as magnetic data storage or magnetic resonance imaging.

© 2007 Elsevier B.V. All rights reserved.

PACS: 81.07.de; 61.80.jh; 61.72.Cc

Keywords: Carbon nanotube (CNT); Cobalt; Magnetism; Superparamagnetism; Nanocrystal; Ion irradiation; Raman; TEM

1. Introduction

Ion and electron irradiation has been demonstrated to be a powerful tool for changing the morphology of nano-structured systems in a controllable manner and for tailoring their mechanical and electronic properties. The examples are irradiation-assisted engineering of carbon [1–5], boron–nitride [6], and silicon [7] nano-structured materials, as well as patterning or ordering of the magnetic properties of ultrathin metallic ferromagnetic films [8] and self-organization of ensembles of embedded nano-clusters due to the inverse Ostwald ripening effect [9].

The current intensive research of irradiation effects in nanosystems is motivated by not only practical aspects of materials processing, but also the fundamental aspects of understanding the response of such systems to irradiation. Indeed, many fascinating irradiation-induced phenomena

inherently related to the nanometer-size of the systems have been reported, such as pressure buildup inside irradiated carbon onions [10,11] and nanotubes [12,13]. It was demonstrated that both electron and ion irradiation can give rise to this effect, and that the pressure can be as high as 30 GPa, so that diamond crystals can nucleate inside onions, while foreign materials encapsulated inside nanotubes can be deformed and extruded. High temperatures were shown to be important for this effect to occur at electron irradiation [12]. As for ion bombardment of nanotubes, high-energy (100 MeV) ions have been demonstrated to result in pressure buildup at room temperature [13]. This raises two questions: what would be the response of nanotubes to irradiation at lower ion energies and what is the role of temperature?

In this work, we use ion irradiation combined with transmission electron microscopy (TEM) and Raman characterization of the irradiated samples to study the response of multi-walled carbon nanotubes (MWNTs) encapsulating cobalt nanorods to ion irradiation at

*Corresponding author. Tel.: +358 503797555.

E-mail address: ossi.lehtinen@helsinki.fi (O. Lehtinen).

different temperatures. We use various ions (C, H, He) and medium ion energies (40–500 keV), as this ion energy range would be easily accessible in technological applications.

The choice of cobalt as the material encapsulated inside carbon nanotubes (CNTs) is motivated by interesting magnetic properties of composite cobalt–carbon nanomaterials [14–16], which are of great interest for various applications such as magnetic data storage, ferrofluids, or magnetic resonance imaging.

2. Experimental procedure

2.1. Sample preparation

The samples consisted of MWNTs encapsulating cobalt nanorods which were produced by means of a modified ethanol–metallocene deposition process, as described in detail in Ref. [12]. In addition to nanotubes, the samples contained a certain amount of carbon onions, and isolated metal particles. The nanotubes were dispersed ultrasonically in ethanol and placed onto Mo TEM grids for carrying out electron microscopy and ion irradiation experiments.

2.2. Ion irradiation

The accelerator used for this study was a 500 kV implanter of the Accelerator Laboratory producing ion beams with a large selection of atomic species and adjustable energy from 10 to 500 keV.

The samples were mounted on a heating stage where the sample temperature could be adjusted from room temperature to 800 °C. For the ion current used (approx. 0.1–5 $\mu\text{A}/\text{cm}^2$), the effects of irradiation on heating were estimated to be negligible. The purpose of heating the samples while irradiating was to facilitate the self-healing property [12] of CNTs at elevated temperatures. A beam sweeping unit was used to produce a homogeneous distribution of ions in the sample from a focused ion beam. The sweeping unit can raster the beam in the desired area of approximately 10 cm^2 by varying voltages in electric deviator plates in both x and y directions.

Four Faraday cups with well-defined surface areas were placed in front of the sample. As the beam was swept over both the sample and the Faraday cups, the irradiation dose could be determined from the charge accumulated in the cups. Different irradiation doses, energies, and temperatures were used on the samples, and these are summarized in Table 1.

2.3. High resolution TEM

The samples were examined in a high resolution TEM (FEI Tecnai F-30) of the Mainz University with a field emission gun and an acceleration voltage of 300 kV before and after ion irradiation. A current density of 30 A/cm^2 was used in the electron irradiation. This had a negligible

Table 1

The samples, ions, ion energies, temperatures, doses used in the experiments, as well as displacements per atom (DPA) and ratio of the intensities of D and G bands obtained from Raman characterization

Sample no.	Ion	Energy (keV)	T (°C)	Dose (ion/ cm^2)	DPA	D/G ratio
1	C	40	800	1.8e16	2.5	0.70
2	C	40	500	6.0e16	8.3	–
3	C	380	500	1.0e17	1.6	0.56
4	C	350	500	1.0e18	17	0.71
5	H	350	800	3.0e17	0.02	0.63
6	He	350	800	1.0e19	7.9	0.83

effect on the sample. In addition, a non-irradiated sample was heated up to 800 °C and examined both before and after heating with the TEM. This was to distinguish heating and irradiation effects.

2.4. Raman spectroscopy

The Raman measurements were carried out using a single-stage spectrometer (Acton SpectraPro 500I, resolution 10 cm^{-1}) of the Laboratory of Physical Chemistry equipped with a charge-coupled device camera (Andor InstaSpec IV) and an Ar+ laser (Omnichrome 543-AP, 100 mW at 514.5 nm). The laser radiation was focused to the sample surface, and Raman light was detected in the transverse direction without polarization analysis. More details of the experimental procedures can be found elsewhere [17].

3. Results and discussion

The typical low and high magnification TEM images of the samples taken before irradiation are shown in Fig. 1(a) and (b). Co rods encapsulated inside the hollow of the tubes are clearly observable. In addition to those, isolated cobalt clusters are seen as well.

Although TEM evidenced the presence of amorphous carbon and graphitic particles in the samples, the pristine samples had a well-ordered structure, as Raman spectra of the samples showed very weak intensity of the D band, Fig. 2, which is normally associated with defects [18].

The irradiation with carbon ions at all temperatures dramatically changed the morphology of the system. Fig. 1((c) and (d)) show the typical images of nanotubes in samples 4 and 1, respectively. It is evident that irradiation gave rise to strong amorphization of the carbon network, especially for sample 4. To quantitatively characterize the damage, we estimated the DPA (displacements per atom) rate in the samples using the computer program TRIM 2003 [19], which is a Monte Carlo simulation of the interaction of energetic ions and matter. The DPA value describes how many times each atom in the target was displaced under irradiation. The higher damage

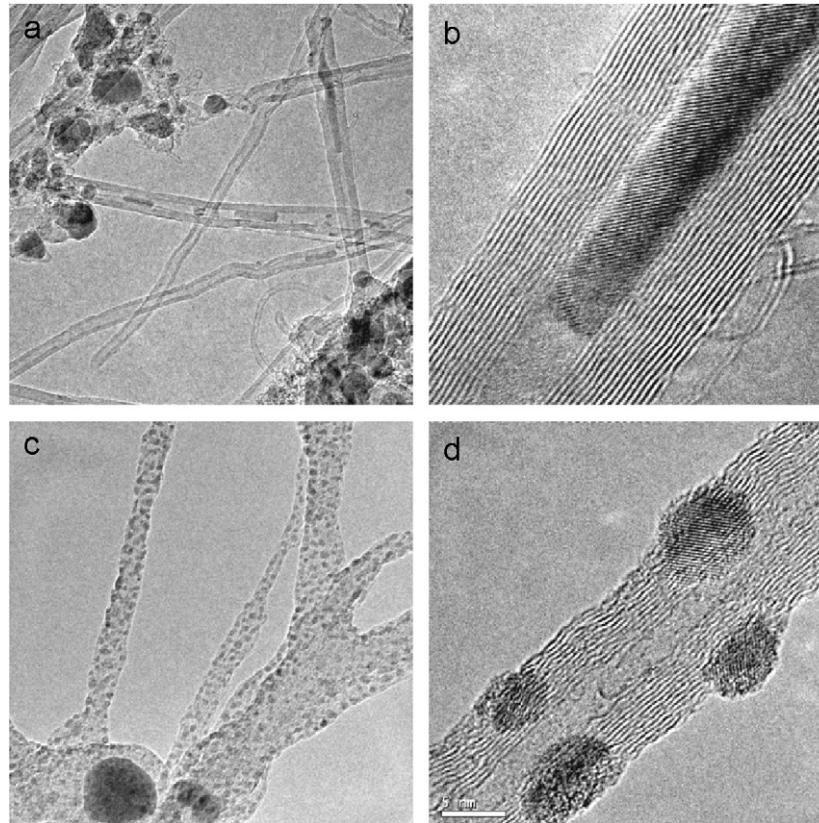


Fig. 1. Typical low and high magnification transmission electron microscopy images of Co-nanotube samples before (a,b) and after (c,d) ion irradiation. Image (c) corresponds to sample (4) and image (d) to sample (1).

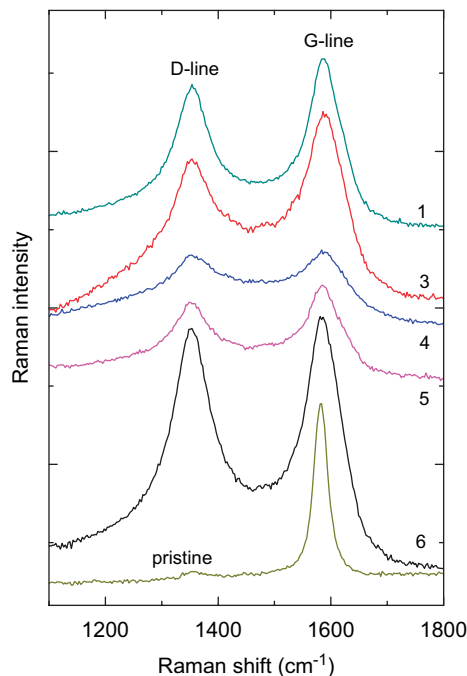


Fig. 2. Raman spectra of the pristine and irradiated carbon nanotubes encapsulating Co nanoclusters. The sample specification is listed in Table 1. Ion irradiation resulted in amorphization of the carbon network as evidenced by an increase in the ratio of the intensities of the D and G bands. The effect is partly smeared out as irradiation was carried out at high temperatures.

in sample 4 is clearly due to higher irradiation dose and thus higher DPA values.

We stress that keeping the sample at high temperatures could not prevent the accumulation of the damage. This is in a sharp contrast to electron irradiation of CNTs: the experiments [20,21] showed that electron irradiation of nanotubes at temperatures exceeding 600 °C gives rise to the shrinkage of the irradiated nanotubes due to atom sputtering [22] and defect migration [23,24], but the shells remain coherent and preserve their tubular structure. Such a difference can be understood by a different mechanism of energy transfer from the projectile to the target atom: electron irradiation creates mostly *isolated* single vacancies, while heavy ions like C for the energy range studied give rise to several nearby single- [25] and multi-vacancies [26] as well as local amorphous regions due to a higher momentum of the recoil atoms and thus a bigger role of collisional cascades. As for high energies (100 MeV) used in Ref. [13], the energy transfer from the projectile to the target is essentially due to electronic stopping, which results mostly in the local heating of the sample accompanied by creation of a certain number of single vacancies. The amount of damage in nanotubes irradiated with C ions inferred from the shape of the Raman spectra overall matched the TEM results and the estimated DPA ratio, see the table. For sample 5 irradiated with H, the D/G ratio proved to be unexpectedly high. We would

like to point out that in previous experiments on proton irradiation of CNTs [27,28] amorphization of nanotubes at irradiation doses less than 3×10^{17} ions/cm² was reported as well, consistently with our experiments. Further studies are required to fully understand the response of nanotubes to irradiation with light ions. The contradiction between the estimated and actual damage may indicate that the temperature distribution was non-uniform during the irradiation.

Careful analysis of the samples showed no evidence for compression effects, even at moderate irradiation dose and low DPA, as for sample 5, when the nanotube and rod integrity was preserved in the most of the sample. At high irradiation doses Co nanorods were destroyed and transformed to Co nanoclusters with diameters of about several nm encapsulated in amorphous carbon rods. The big cluster at the bottom of the Fig. 1 appeared during the sample preparation. A considerable number of clusters were found on the surface of the fibers as well. Such transformations can be understood by heavy damage and strong momentum transfer to metal atoms from the impinging ions: the metal atoms may have been displaced through big holes in the nanotube walls created by ion impacts. Interestingly enough, high temperatures did not result in the coalescence of Co clusters, probably due to the inverse Ostwald ripening effect [9]. This may also be the reason for a relatively uniform size of the clusters around 4 nm.

The produced cobalt clusters embedded into the amorphous carbon matrix resemble structures described in the literature [14–16] and thus may have useful magnetic properties to be studied in the future. If it is indeed the case, our method could provide a way to create quasi-one-dimensional strips of ferromagnetic nano particles embedded onto amorphous matrix.

4. Conclusions

Our irradiation experiments on nanotubes encapsulated with Co rods with medium ion energies (40–500 keV) combined with TEM and Raman characterization of the irradiated samples showed no evidence for compression effects reported for electron and high-energy (100 MeV) ion irradiation. Instead, ion bombardment transformed the nanotubes to amorphous carbon matrix with embedded Co clusters having typical diameters of about several nanometers. As Co is magnetic, such one-dimensional composite systems can be used for various applications such as magnetic data storage and magnetic resonance imaging.

Acknowledgments

The research was supported by the Academy of Finland under its Centres of Excellence Program (Computational Molecular Science) and projects NANOTOMO (118055) and MEPNAS (111469) and the FinnNano program.

References

- [1] A. Kis, G. Csányi, J.-P. Salvetat, T.-N. Lee, E. Couteau, A.J. Kulik, W. Benoit, J. Brugger, L. Fórró, *Nature Mater.* 3 (2004) 153.
- [2] G. Gómez-Navarro, P.J. De Pablo, J. Gómez-Herrero, B. Biel, F.J. Garcia-Vidal, A. Rubio, F. Flores, *Nature Mater.* 4 (2005) 534.
- [3] M. Terrones, H. Terrones, F. Banhart, J.-C. Charlier, P.M. Ajayan, *Science* 288 (2000) 1226.
- [4] A. Hashimoto, K. Suenaga, A. Gloter, K. Urita, S. Iijima, *Nature* 430 (2004) 870.
- [5] M. Terrones, F. Banhart, N. Grobert, J.-C. Charlier, H. Terrones, P.M. Ajayan, *Phys. Rev. Lett.* 89 (2002) 075505.
- [6] D. Golberg, Y. Bando, *Recent Res. Dev. Appl. Phys.* 2 (1999) 1.
- [7] S. Xu, M. Tian, J. Wang, J. Xu, J.M. Redwing, M.H.W. Chan, *Small* 1 (2005) 1221.
- [8] C. Chappert, H. Bernas, J. Ferreacut, V. Kottler, J. Jamet, Y. Chen, E. Cambriil, T. Devolder, F. Rousseaux, V. Mathet, H. Launois, *Science* 280 (5371) (1998) 1919.
- [9] K.H. Heinig, T. Muller, B. Schmidt, M. Strobel, W. Möller, *Appl. Phys. A Mater. Sci. Process.* 77 (2003) 17.
- [10] F. Banhart, P.M. Ajayan, *Nature* 382 (1996) 433–435.
- [11] P. Wesolowski, Y. Lyutovich, F. Banhart, H.D. Carstanjen, H. Kronmüller, *Appl. Phys. Lett.* 71 (1997) 1948.
- [12] L. Sun, F. Banhart, A.V. Krasheninnikov, J.A. Rodríguez-Manzo, M. Terrones, P.M. Ajayan, *Science* 312 (2006) 1199.
- [13] A. Misra, P.K. Tyagi, M.K. Singh, D.S. Misra, J. Ghatak, P.V. Satyam, D.K. Avasthi, *Diamond Relat. Mater.* 15 (2006) 300.
- [14] M.E. McHenry, S.A. Majetich, J.O. Artman, M. DeGraef, S.W. Staley, *Phys. Rev. B* 49 (1994) 11358.
- [15] S. Tomita, M. Hikita, M. Fujii, S. Hayashi, K. Akamatsu, S. Deki, Y. Yasuda, *J. Appl. Phys.* 88 (2000) 5452.
- [16] M.E. McHenry, D.E. Laughlin, *Acta Mater.* 48 (1999) 223.
- [17] L. Khriachtchev, *Top. Appl. Phys.* 100 (2006) 403.
- [18] A.C. Ferrari, J. Robertson, *Phil. Trans. R. Soc. A* 362 (2004) 2269.
- [19] J.F. Ziegler, J.P. Biersack, Program TRIM, 2003. (<http://www.srim.org>).
- [20] F. Banhart, *Rep. Prog. Phys.* 62 (1999) 1181.
- [21] F. Banhart, J.X. Li, A.V. Krasheninnikov, *Phys. Rev. B* 71 (2005) 241408(R).
- [22] A.V. Krasheninnikov, F. Banhart, J.X. Li, A. Foster, R. Nieminen, *Phys. Rev. B* 72 (2005) 125428.
- [23] A.V. Krasheninnikov, P.O. Lehtinen, A.S. Foster, R.M. Nieminen, *Chem. Phys. Lett.* 418 (2006) 132.
- [24] A.V. Krasheninnikov, K. Nordlund, P.O. Lehtinen, A.S. Foster, A. Ayuela, R.M. Nieminen, *Phys. Rev. B* 69 (2004) 073402.
- [25] A.V. Krasheninnikov, *Solid State Commun.* 118 (2001) 361.
- [26] J. Kotakoski, A.V. Krasheninnikov, K. Nordlund, *Phys. Rev. B* 74 (2006) 245420.
- [27] V.A. Basiuk, K. Kobayashi, T.K.Y. Negishi, E.V. Basiuk, J.M. Saniger-Blesa, *Nano Lett.* 2 (2002) 789.
- [28] P.P. Neupane, M.O. Manasreh, B.D. Weaver, B.J. Landi, R.P. Raffaele, *Appl. Phys. Lett.* 86 (2005) 221908.